

# Visual tracing of diffusion and biodistribution for amphiphilic cationic nanoparticles using photoacoustic imaging after ex vivo intravitreal injections

Xu Xu\*

Zhaokang Xu\*

Junyi Liu

Zhaoliang Zhang

Hao Chen

Xingyi Li

Shuai Shi

Institute of Biomedical Engineering,  
School of Ophthalmology &  
Optometry and Eye Hospital,  
Wenzhou Medical University,  
Wenzhou, Zhejiang, People's Republic  
of China

\*These authors contributed equally  
to this work

**Abstract:** To visually trace the diffusion and biodistribution of amphiphilic cation micelles after vitreous injection, various triblock copolymers of monomethoxy poly(ethylene glycol)–poly(ε-caprolactone)–polyethylenimine were synthesized with different structures of hydrophilic and hydrophobic segments, followed by labeling with near-infrared fluorescent dye Cyanine5 or Cyanine7. The micellar size, polydispersity index, and surface charge were measured by dynamic light scattering. The diffusion was monitored using photoacoustic imaging in real time after intra-vitreous injections. Moreover, the labeled nanoparticle distribution in the posterior segment of the eye was imaged histologically by confocal microscopy. The results showed that the hydrophilic segment increased vitreous diffusion, while a positive charge on the particle surface hindered diffusion. In addition, the particles diffused through the retinal layers and were enriched in the retinal pigment epithelial layer. This work tried to study the diffusion rate via a simple method by using visible images, and then provided basic data for the development of intraocular drug carriers.

**Keywords:** visible tracing, cavum vitreum, biodistribution, diffusion rate

## Introduction

Diabetic retinopathy, age-related macular degeneration, and uveitis are disorders that significantly impact vision and the quality of life.<sup>1,2</sup> To treat these disorders, most drugs need sustained and effective delivery to the posterior segment of the eye.<sup>3</sup>

This part of the eye is composed of a blood–retinal barrier and an inner retinal limiting membrane that are relatively impermeable to many therapeutic agents. To improve the effectiveness of the drugs, invasive local therapy such as intravitreal injection is generally required. Intravitreal injections have been considered the preferred route of drug delivery to the eye during the past 2 decades, and they are the most effective drug delivery method for the retina.<sup>4–7</sup> Compared with systemic administration, this method has the advantages of localizing the drug effect with higher drug concentrations in the vitreous and retina. It is commonly performed by injecting a drug suspension or solution into the vitreous cavity in the center of the eye via pars plana using a 30 G needle.

With recent advances in nanomedicine, many carriers have potential applications during the process of ocular drug delivery.<sup>8–11</sup> A series of drug carriers based on poly(ethylene glycol)–poly(ε-caprolactone) (PEG-PCL) and poly(ethylene glycol)–poly(L-lactide-co-glycolide) amphiphilic nanoparticles (NPs) have been exploited for more efficient drug delivery via intravitreal administration.<sup>12–15</sup> They are considered essential for overcoming the current limitations by facilitating frequent and sustained release of retinal medications.

Correspondence: Xingyi Li; Shuai Shi  
Institute of Biomedical Engineering,  
School of Ophthalmology & Optometry  
and Eye Hospital, Wenzhou Medical  
University, 270 Xueyuan Road, Wenzhou  
325027, People's Republic of China  
Tel/fax +86 577 8883 3806  
Email [lixingyi\\_1984@163.com](mailto:lixingyi_1984@163.com);  
[shuaishi23@163.com](mailto:shuaishi23@163.com)

Their properties, including particle size, surface charge, and segment formation, affect diffusion efficiency and distribution in the posterior segment of the eye.<sup>10,16,17</sup> Based upon these properties, in this study, we characterized the effects of hydrophilic segments on the diffusion and tissue distribution after a single intravitreal injection.

## Experimental methods

### Animals and materials

Japanese albino rabbits and female Sprague Dawley rats (weighing ~200 g) were purchased from the Laboratory Center of Wenzhou Medical University (Wenzhou, People's Republic of China). All animal care and experimental procedures were conducted according to the Institutional Animal Care and Use Guidelines of Wenzhou Medicine University and the Guide for the Care and Use of Laboratory Animals, Institute of Laboratory Animal Resources. Ethical approval was given by the Medical Ethics Committee of School of Ophthalmology & Optometry and Eye Hospital (Wenzhou Medical University) with the following reference number: KYK(2014)33.

Reagents included monomethoxy poly(ethylene glycol) (MPEG, Mn 5,000 and 2,000; Sigma-Aldrich Co., St Louis, MO, USA),  $\epsilon$ -caprolactone ( $\epsilon$ -CL, MW 114; Alfa Aesar, Ward Hill, MA, USA), polyethylenimine (PEI, MW 2,000; Sigma-Aldrich Co.), stannous octoate ( $\text{Sn}(\text{Oct})_2$ ; Sigma-Aldrich Co.), amine reactive Cyanine5 (Cy5<sup>®</sup>, Cy5-NHS) and Cyanine7 (Cy7<sup>®</sup>, Cy7-NHS) dyes (Lumiprobe, Hannover, Germany), and acryloyl chloride (Sigma-Aldrich Co.). Methanol, ethanol, and diethyl ether were purchased from Wuxi JiaNi Chemicals (Wuxi, People's Republic of China). All reagents and solvents were of analytical grade.

### Synthesis of Cy-labeled amphiphilic copolymers

Various MPEG-PCL-g-PEIs with different block formations were synthesized according to previous reports.<sup>18,19</sup> Briefly, MPEG-PCL with designed formations was synthesized using ring-opening polymerization of  $\epsilon$ -CL initiated by PEG2000 or PEG5000. After being modified by acryloyl chloride at the end of the PCL, the copolymer MPEG-PCL-C=C was added to a PEI2000 solution in methanol, drop by drop, and stirred for 24 hours at 50°C to complete the reaction. The products were purified by dialysis and then lyophilized. By mixing Cy7-NHS or Cy5-NHS with triblock copolymer MPEG-PCL-g-PEI in an aqueous solution at room temperature, the self-assembled NPs were labeled with the fluorescent probe. The excess probes were removed by dialysis within 48 hours.

### Preparation and characterization of self-assembled NPs

All synthesized copolymers were amphiphilic, and their NPs were prepared using the self-assembly method in aqueous solution at temperatures >55°C. Particle size distribution, polydispersity index, and the zeta potential of NPs were measured by dynamic light scattering, using a Zeta Sizer (NanoZS; Malvern Instruments, Malvern, UK). The critical micelle concentration was determined by fluorescence measurements using pyrene as the fluorescent probe at 25°C.<sup>18</sup> The excitation wavelength was 333 nm with a scanning speed 500 nm/min, and the emission fluorescence was monitored at 373 nm and 384 nm. The critical micelle concentration was estimated by analysis of the ratio of intensities at 373–384 nm (I373/I384). To determine labeling with a fluorophore, a fluorescence spectra assay of Cy7/Cy5-labeled NPs was measured using a fluorescence spectrometer (LS55; PerkinElmer Inc., Waltham, MA, USA).

The cytotoxicity of the mPEG-PCL-g-PEI NPs was evaluated by 3-(4,5-dimethylthiazol-2-yl)-2,5-diphenyltetrazolium bromide (MTT) assay. ARPE cells were seeded in 96-well plates at a density of  $4 \times 10^4$  cells/well in 100  $\mu\text{L}$  of growth medium and incubated 24 hours, and then 100  $\mu\text{L}$  of a series of mPEG-PCL-g-PEI NPs at different concentrations were added. After incubating the cells for a further 24 hours, 10% Cell Counting Kit 8 was added. All absorbances were measured at 450 nm using a Spectramax microplate reader (Molecular Devices LLC, Sunnyvale, CA, USA), and untreated cells were used as controls.

### Intravitreal injections

Cy-labeled MPEG-PCL-g-PEI NPs were prepared by dissolving the copolymer in water at 60°C, and after self-assembly, the solution was filtered using a 0.22  $\mu\text{m}$  membrane filter before in vivo injection. Sprague Dawley rats (female, 4–8 weeks old) were anesthetized by intraperitoneal injection of 100 mg/kg ketamine and 10 mg/kg xylazine. Both eyes were injected intravitreally with 3  $\mu\text{L}$  of Cy5-labeled amphiphilic copolymer using a 33 G syringe (Hamilton, Reno, NV, USA) into a quadrant posterior to the limbus.

### Photoacoustic imaging ex vivo

The eyes of Japanese albino rabbits were enucleated and divided into four groups, including a Cy7-labeled MPEG2000-PCL2000-g-PEI2000 (2-2-2) group, a Cy7-labeled MPEG5000-PCL2000-g-PEI2000 (5-2-2) group, a Cy7-labeled MPEG2000-PCL6000-g-PEI2000

(2-6-2) group, and a free Cy7 group. Each of the eyes received an intravitreal injection of 20  $\mu$ L of the above-mentioned micelle solutions (5 mg/mL). Photoacoustic (PA) imaging at 1, 10, and 18 minutes after injection was performed using a preclinical PA computerized tomography scanner (Nexus 128; Endra, Inc., Ann Arbor, MI, USA). A freshly enucleated eye was used for PA imaging before intravitreal injection and was designated as 0 minutes in each group. Three eyes were used for each treatment (or control) group at each time point.

## Histology

Twenty-four rats were divided into three groups: a PEG5000-PCL2000-g-PEI2000 (5-2-2) group, a PEG2000-PCL2000-g-PEI2000 (2-2-2) group, and a PEG2000-PCL6000-g-PEI2000 (2-6-2) group. The Cy5-labeled MPEG-PCL-g-PEI polymer micelles were intravitreally injected into each rat group (2  $\mu$ L, 5 mg/mL). At 1, 3, 5, and 7 days, three rats were killed by injection of a lethal dose of pentobarbital, and the eyes were enucleated and fixed overnight in 4% paraformaldehyde, followed by dehydration overnight in 30% sucrose solution. The ocular globes were embedded in Tissue-Tek OTC compound (Sakura FineTechnical, Tokyo, Japan) and stored frozen at  $-80^{\circ}\text{C}$ . The tissue was sectioned into 8  $\mu$ m slices with a vibrating blade microtome (Leica Microsystems, Wetzlar, Germany) and characterized using a fluorescence microscope (QWin; Leica). Three rats (three eyes) were used for each treatment group at each time point (36 eyes of 36 rats).

## Results

### Characterization of NPs with different formations

As a triblock copolymer, the formation of MPEG-PCL-g-PEI NPs was adjustable during the synthesis process. Two PEG ligands with molecular weight of 2,000 Da or 5,000 Da were chosen to initiate ring-open reaction with  $\epsilon$ -CL. Ligand PCL with different molecular weights can be synthesized by adding various ratios between PEG and  $\epsilon$ -CL, which eventually adjusts the proportion of hydrophilic and hydrophobic

segments in the amphiphilic polymer. After chemically grafting PEI, we obtained three amphiphilic polymer models, including MPEG2000-PCL2000-g-PEI2000 (2-2-2), MPEG5000-PCL2000-g-PEI2000 (5-2-2), and MPEG2000-PCL6000-g-PEI2000 (2-6-2). To assess the effect of micelle formulation conditions, the size distribution and particle zeta potential were characterized using dynamic light scattering and zeta potential analysis, respectively. The results are shown in Table 1. In a similar manner as previously reported, these amphiphilic copolymers could be self-assembled into nanoscale particles with a uniform dispersion (Figure 1A). Particle sizes of the three polymers had no significant difference in the range of 40–62 nm. Owing to the presence of PEI segments, positive charges on three self-assembled micelle surfaces were MPEG2k-PCL2k-g-PEI2k (2-2-2) at  $24.5 \pm 1.67$  mV, MPEG2k-PCL6k-g-PEI2k (2-6-2) at  $32.5 \pm 0.35$  mV, and MPEG5k-PCL2k-g-PEI2k (5-2-2) at  $20.47 \pm 2.74$  mV. Due to a longer hydrophobic segment in MPEG2000-PEG6000-g-PEI, its hydrophobic interactions between PCL segments made it more stable during self-assembling process, and thus, MPEG2000-PEG6000-g-PEI appears to be tenfold more thermodynamically stable based on critical micelle concentration.

After labeling with two fluorochromes, Cy5 and Cy7 (Lumiprobe), fluorescence spectra characterization was performed as shown in Figure 1B. These three polymers were used for pairwise comparisons of vitreous cavity diffusion and tissue distribution after intravitreal injection.

The cytotoxicity increased with increasing concentration of MPEG-PCL-g-PEI micelles (Figure 2). The cell viability of MPEG-PCL-g-PEI with the formation 2k-2k-2k (2-2-2) group decreased to 38% at the concentration of 60  $\mu$ g/mL, while the other two groups had significant cytotoxicity at this concentration. Additionally, the group of 2k-6k-2k micelles formation (2-6-2) showed less toxicity within the concentration of 100  $\mu$ g/mL.

### PA imaging of NP diffusion

These triblock copolymers were labeled with Cy7, so they could be traced by PA imaging (Figures 3 and 4). A blank

**Table 1** Physicochemical characteristics of each MPEG-PCL-g-PEI formulation

Sample	Size <sup>a</sup> (nm), mean $\pm$ SD	PDI <sup>a</sup> , mean $\pm$ SD	Zeta potential (mV), mean $\pm$ SD	CMC <sup>b</sup> (mg/mL)
MPEG 2000 Da-PCL 2000 Da-PEI 2000 Da (2-2-2)	62.73 $\pm$ 0.08	0.198 $\pm$ 0.008	24.5 $\pm$ 1.67	0.05
2-6-2; MPEG 2000 Da-PCL 6000 Da-PEI 2000 Da (2-6-2)	40.79 $\pm$ 0.1	0.18 $\pm$ 0.006	32.5 $\pm$ 0.35	0.005
5-2-2; MPEG 5000 Da-PCL 2000 Da-PEI 2000 Da (5-2-2)	47.19 $\pm$ 0.22	0.22 $\pm$ 0.003	20.47 $\pm$ 2.74	0.03

**Notes:** <sup>a</sup>Determined by dynamic light scattering. <sup>b</sup>Determined by pyrene-based fluorescence spectrometry.

**Abbreviations:** MPEG, monomethoxy poly(ethylene glycol); PCL, poly( $\epsilon$ -caprolactone); PEI, polyethylenimine; PDI, polydispersity index; CMC, critical micelle concentration.

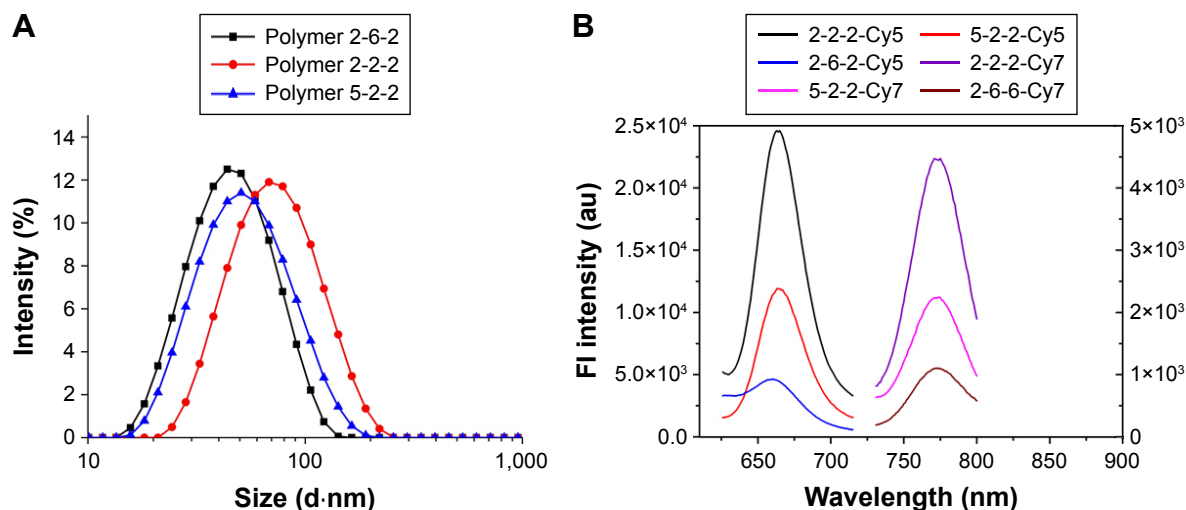


**Figure 1** (A) Size distribution by intensity and (B) fluorescence spectra of the Cy5- and Cy7-labeled micelles (left, emission of Cy5; right, emission of Cy7).

**Abbreviations:** Cy, cyanine; FI, fluorescence; 2-2-2, MPEG 2000 Da-PCL 2000 Da-PEI 2000 Da; 2-6-2, MPEG 2000 Da-PCL 6000 Da-PEI 2000 Da; 5-2-2, MPEG 5000 Da-PCL 2000 Da-PEI 2000 Da.

eye with no injection was used as a control and named “0 minutes”. Owing to the presence of blood vessels in the choroid, significant PA signals were observed in all the control groups. A significant weakening of the Cy7 PA signal from 1 minute to 10 minutes indicated diffusion after the Cy7 vitreous cavity injection. The diffusion of different micelles could be tracked in real time after labeling with Cy7 followed by PA imaging. Figure 4 shows the PA signal intensities (indicated by white circles) of three experimental groups that showed sustained decreases with increasing duration after the injection. The rate of signal weakening corresponded to

the rate of diffusion in the vitreous cavity. When comparing the PA signal intensities at 1 and 18 minutes, the signal weakening rate of the MPEG5000-PCL2000-g-PEI polymer was faster than that in the other two groups, followed by the MPEG2000-PCL2000-g-PEI polymer, then the MPEG2000-PCL6000-g-PEI polymer.

## Biodistribution after intravitreal injection

After injection, all three Cy5-labeled NPs freely diffused throughout the vitreous cavity. The distribution of these NPs was examined by taking fluorescence images at intervals of 1, 3, 5, and 7 days (Figure 5). During the first week after the intravitreal injection, each eye was enucleated and cut into 8  $\mu$ m thick sections. One day after intravitreal injection, fluorescence microscopy showed that the Cy5-labeled NPs had already accumulated preferentially within the retinal pigment epithelial (RPE) cells (Figure 5). With increasing time, the fluorescence intensity of the RPE layer increased (Figure 5), with a maximum intensity on the fifth day (Figure 5). The three polymer compositions had different diffusion rates in the retina.

Next, the kinetics of tissue and cellular localization in the retina of these three amphiphilic self-assembled NPs were followed by semi-quantitative statistics (Figure 6). The confocal fluorescence microscope could quantitate the fluorescence intensity via its own software. This tool was used to evaluate the biodistribution of micelles in each retinal layer. All eight layers of the retina were observed, and the fluorescent intensities of three selected sections in each layer were recorded. The biodistribution and infiltration process of the intravitreally injected NPs were

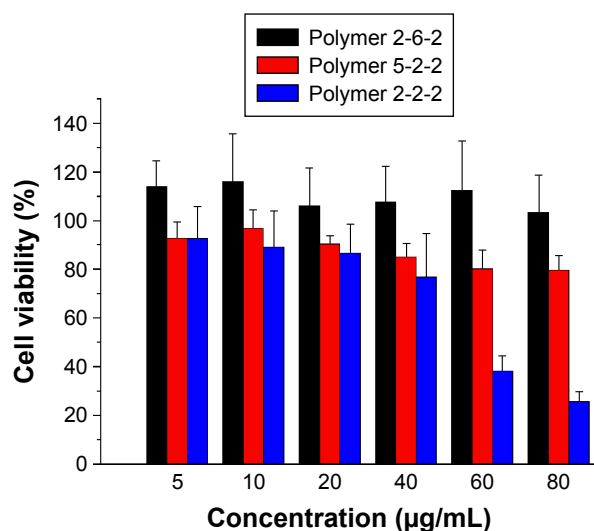


**Figure 2** Cytotoxicity of MPEG-PCL-g-PEI micelles of various compositions on ARPE cells and cell viability were determined by MTT assay (n=6).

**Abbreviations:** MPEG, monomethoxy poly(ethylene glycol); PCL, poly( $\epsilon$ -caprolactone); PEI, polyethylenimine; MTT, 3-(4,5-dimethylthiazol-2-yl)-2,5-diphenyltetrazolium bromide; 2-2-2, MPEG 2000 Da-PCL 2000 Da-PEI 2000 Da; 2-6-2, MPEG 2000 Da-PCL 6000 Da-PEI 2000 Da; 5-2-2, MPEG 5000 Da-PCL 2000 Da-PEI 2000 Da.



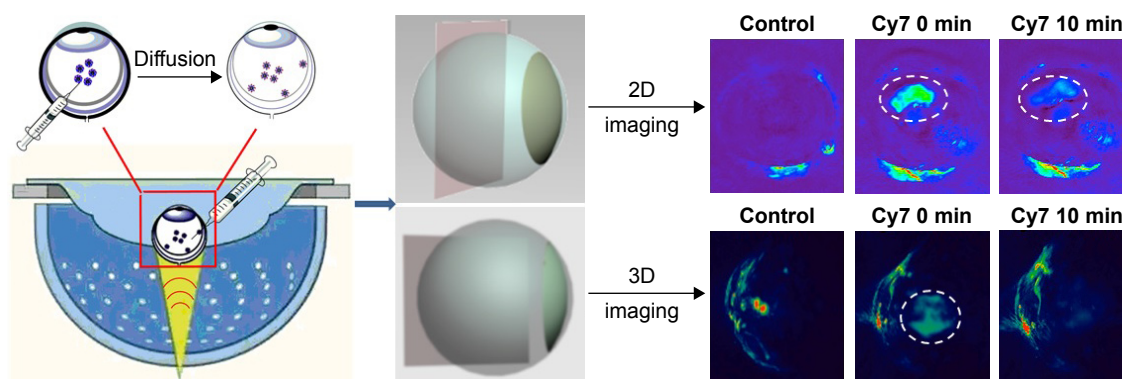


**Figure 3** PA imaging scheme of free Cy7 in enucleated eyes both in 2D/3D view after rabbit vitreous cavity injection.

**Notes:** Free Cy7 with a 3D view at 0, 1, and 10 minutes. The red fluorescence signals might be blood vessels with nonspecific PA signals in eyes. White circles designate the generated PA signal areas of Cy7.

**Abbreviations:** PA, photoacoustic; Cy, cyanine; 2D, two-dimensional; 3D, three-dimensional; min, minutes.

indirectly detected by changes in fluorescence intensity. Figure 5 shows that cationic NPs permeated the retina continually, with a maximum fluorescence on the fourth day (Figure 6C).

## Discussion

With advances in bionanotechnology, a variety of polymeric controlled release systems have been developed for delivery of drugs to the posterior segment of the eye. These systems

include degradable polymeric NPs, polypeptide hydrogel, block copolymer micelles, and ocular implants. They were developed to minimize the frequency of injection and increase drug targeting to specific target sites. As an intraocular administration, intravitreal injections are a more clinically applicable and practical route than subretinal injections.<sup>10,20</sup> Therefore, the relationship between small NP compositions and the diffusion and distribution after intravitreal injection of small NPs is very important.

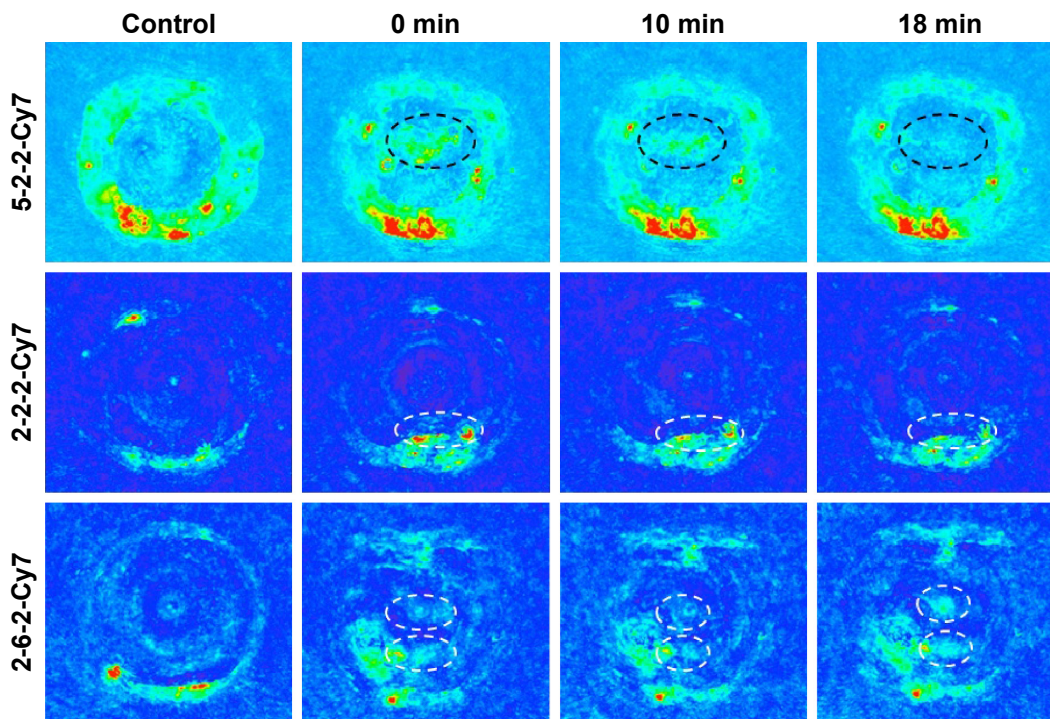


**Figure 4** PA imaging of Cy7-labeled MPEG-PCL-g-PEI micelles in enucleated eyes.

**Notes:** The red fluorescence signals might be blood vessels with nonspecific PA signals in the eyes. White and black circles designate the generated PA signal areas of Cy7-labeled amphiphilic micelles.

**Abbreviations:** PA, photoacoustic; Cy, cyanine; MPEG, monomethoxy poly(ethylene glycol); PCL, poly( $\epsilon$ -caprolactone); PEI, polyethylenimine; min, minutes; 2-2-2, MPEG 2000 Da-PCL 2000 Da-PEI 2000 Da; 2-6-2, MPEG 2000 Da-PCL 6000 Da-PEI 2000 Da; 5-2-2, MPEG 5000 Da-PCL 2000 Da-PEI 2000 Da.

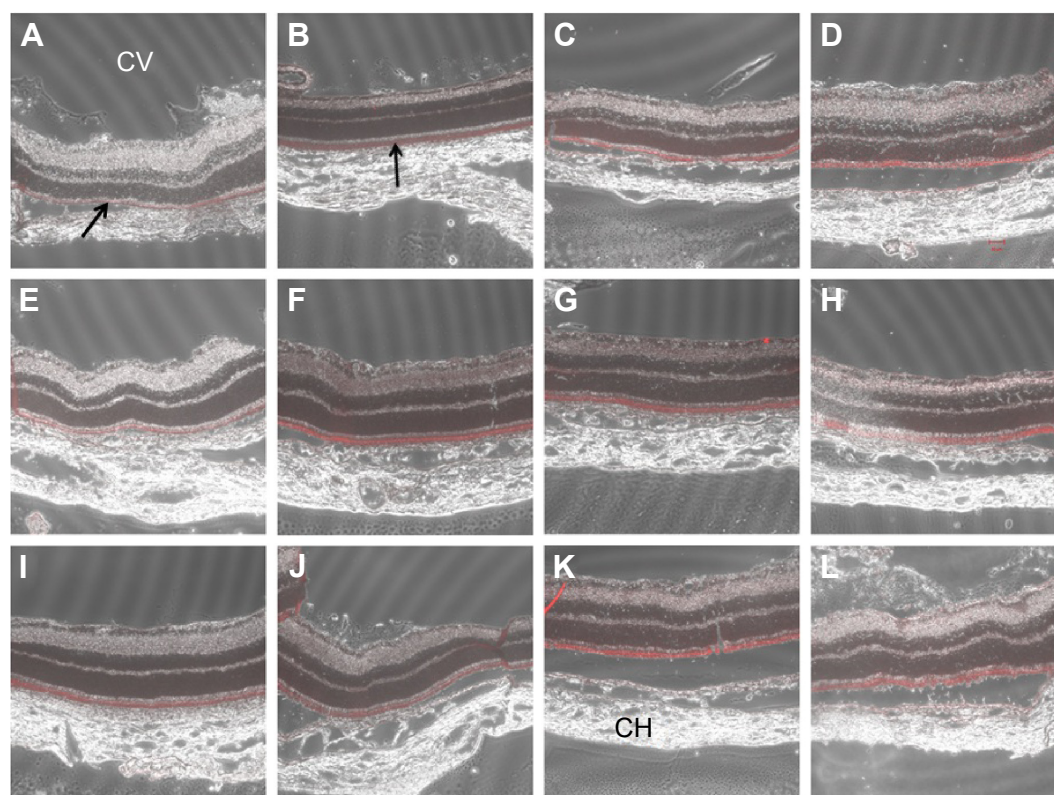


**Figure 5** Confocal microscopy of the retina at 1 day (A, E, and I), 3 days (B, F, and J), 5 days (C, G, and K), and 7 days (D, H, and L) after intravitreal injection of Cy5-labeled micelles in rat. (A–D) Eyes injected with Cy5-labeled MPEG2000 Da-PCL2000 Da-g-PEI micelles. (E–H) Eyes injected with Cy5-labeled MPEG2000 Da-PCL6000 Da-g-PEI micelles. (I–L) Eyes injected with Cy5-labeled MPEG5000 Da-PCL2000 Da-g-PEI micelles. The fluorescent micelles diffused through the retinal layers and were concentrated in the RPE layer. Black arrows indicate this layer.

**Abbreviations:** Cy, cyanine; MPEG, monomethoxy poly(ethylene glycol); PCL, poly( $\epsilon$ -caprolactone); PEI, polyethylenimine; CH, choroid; RPE, retinal pigment epithelium.

In a previous study by Shi et al,<sup>18</sup> MPEG-PCL-g-PEI copolymers with various compositions were used as gene and drug co-delivery vectors. In this study, three composite micelles with various hydrophobic and hydrophilic ligands were used to study the relationship between diffusion rate and their composition. These micelles had similar particle size, which can be diffused freely in the vitreous cavity. However, MPEG2000-PEG2000-g-PEI has the largest particle size. In MPEG2000-PEG2000-g-PEI, the hydrophobic segment is relatively short, and thus, the self-assembly force is less than the other two polymers. On the other hand, as PEI is hydrophilic, it can appear at the hydrophilic shell rather than the hydrophobic core of these self-assembled micelles.

In this study, we used PA imaging, a widely used method in cancer research, to monitor the diffusion of injected Cy7-labeled triblock amphiphilic polymers in the vitreous cavity in real time. By comparing the images before and after injection, the PA signal areas were determined, and the changes of fluorescence intensity in the PA images represented the diffusion of Cy7-labeled polymers (Figure 2).

After the vitreous cavity, slices of rat retina were used to evaluate the biodistribution, while PA images using rabbit were used to study the diffusion rate. Two experiments made full use of the existing experimental conditions, and their results can be complementary to each other. Two results confirmed that the copolymer MPEG-PCL-g-PEI could be quickly dispersed through retinal cell layers and enriched into RPE layer after intravitreal injection.

Three block copolymers (MPEG5000-PCL2000-g-PEI, MPEG2000-PCL2000-g-PEI, and MPEG2000-PCL6000-g-PEI) could self-assemble into NPs with similar sizes and different surface charges. In the three polymer PA images of Figure 3, MPEG5000-PCL2000-g-PEI with the longest PEG segments and  $20.47 \pm 2.74$  mV surface charges had the most obvious changes in PA signals. By comparing the signal changes in the eye injected with MPEG2000-PCL2000-g-PEI or MPEG2000-PCL6000-g-PEI, the results shown in Figure 3 indicate that a hydrophilic segment on the particle surface enhanced the diffusion efficiency of the particle after intravitreal injection.

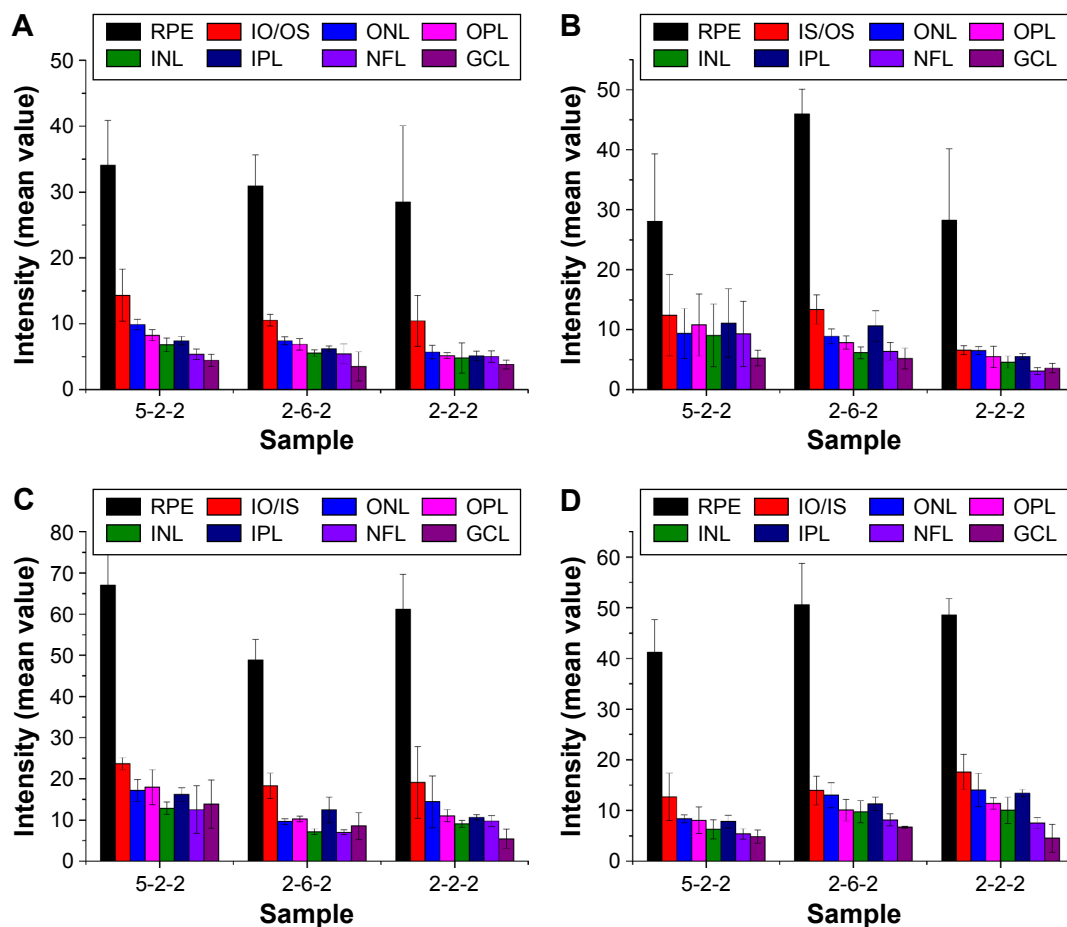


**Figure 6** Biodistribution of MPEG-PCL-g-PEI NPs after intravitreal injection at each time point (A) 1 day, (B) 3 days, (C) 5 days, and (D) 7 days.

**Note:** The bar graphs were obtained from confocal microscopic images of whole eye cryosections.

**Abbreviations:** MPEG, monomethoxy poly(ethylene glycol); PCL, poly( $\epsilon$ -caprolactone); PEI, polyethylenimine; NPs, nanoparticles; RPE, retinal pigment epithelium; INL, inner nuclear layer; IPL, inner plexiform layer; OPL, outer plexiform layer; ONL, outer nuclear layer; NFL, nerve fiber layer; GCL, ganglion cell layer; IO/IS, inner segment of photoreceptor/outer segment of photoreceptor; 2-2-2, MPEG 2000 Da-PCL 2000 Da-PEI 2000 Da; 2-6-2, MPEG 2000 Da-PCL 6000 Da-PEI 2000 Da; 5-2-2, MPEG 5000 Da-PCL 2000 Da-PEI 2000 Da.

A different rate of diffusion between the group injected with MPEG2000-PCL2000-g-PEI and MPEG2000-PCL6000-g-PEI might be due to their different surface charges. MPEG2000-PCL2000-g-PEI could self-assemble into 62 nm NPs and with 24 mV surface charges, while MPEG2000-PCL6000-g-PEI NPs assembled into 40 nm particles with a 32 mV zeta potential. These three self-assembled NPs with sizes <100 nm can diffuse freely in vitreous (Table 1). Thus, a strongly positive charge (>30 mV) on the particle surface has no effect on diffusion after intravitreal injection.

## Conclusion

Hydrophilic segments on the surface of amphiphilic self-assembled NPs improved their diffusion after intravitreal injection. A positive charge did not affect the rate of diffusion. The cationic amphiphilic polymer quickly reached the retina and was concentrated in RPE cells.

## Acknowledgments

The authors are grateful to Doctors Zonghai Shen and Dehong Hu from the Institute of Biomedicine and Biotechnology at Shenzhen Institutes of Advanced Technology for excellent technical assistance of PA imaging studies. The research was supported by the National Natural Science Foundation of China (Grant number NSFC51303203), Science and Technology Planning Project of Wenzhou City (number Y20140144).

## Disclosure

The authors report no conflicts of interest in this work.

## References

- Kim YC, Chiang B, Wu X, Prausnitz MR. Ocular delivery of macromolecules. *J Control Release*. 2014;190:172–181.
- Keles S, Halici Z, Atmaca HT, et al. The ocular endothelin system: a novel target for the treatment of endotoxin-induced uveitis with bosentan. *Invest Ophthalmol Vis Sci*. 2014;55(6):3517–3524.



3. Yasin MN, Svirskis D, Seyfoddin A, Rupenthal ID. Implants for drug delivery to the posterior segment of the eye: a focus on stimuli-responsive and tunable release systems. *J Control Release*. 2014;196:208–221.
4. Jager RD, Aiello LP, Patel SC, Cunningham ET Jr. Risks of intravitreal injection: a comprehensive review. *Retina*. 2004;24(5):676–698.
5. Scott IU, Flynn HW Jr. Intravitreal injections: guidelines to minimize the risk of endophthalmitis. In: Jousen AM, Gardner TW, Kirchhof B, Ryan SJ, editors. *Retinal Vascular Disease*. Berlin: Springer; 2007: 283–288.
6. Rawas-Qalaji M, Williams C-A. Advances in ocular drug delivery. *Curr Eye Res*. 2012;37(5):345–356.
7. Rowe-Rendleman CL, Durazo SA, Kompella UB, et al. Drug and gene delivery to the back of the eye: from bench to bedside. *Invest Ophthalmol Vis Sci*. 2014;55(4):2714.
8. Al-Halafi AM. Nanocarriers of nanotechnology in retinal diseases. *Saudi J Ophthalmol*. 2014;28(4):304–309.
9. Huu VA, Luo J, Zhu J, et al. Light-responsive nanoparticle depot to control release of a small molecule angiogenesis inhibitor in the posterior segment of the eye. *J Control Release*. 2015;200:71–77.
10. Bourges JL, Gautier SE, Delie F, et al. Ocular drug delivery targeting the retina and retinal pigment epithelium using polylactide nanoparticles. *Invest Ophthalmol Vis Sci*. 2003;44(8):3562–3569.
11. Reimondez-Troitiño S, Csaba N, Alonso MJ, de la Fuente M. Nanotherapies for the treatment of ocular diseases. *Eur J Pharm Biopharm*. 2015; 95(pt B):279–293.
12. Suen W-LL, Chau Y. Specific uptake of folate-decorated triamcinolone-encapsulating nanoparticles by retinal pigment epithelium cells enhances and prolongs antiangiogenic activity. *J Control Release*. 2013; 167(1):21–28.
13. Yin H, Gong C, Shi S, Liu X, Wei Y, Qian Z. Toxicity evaluation of biodegradable and thermosensitive PEG-PCL-PEG hydrogel as a potential in situ sustained ophthalmic drug delivery system. *J Biomed Mater Res B Appl Biomater*. 2010;92(1):129–137.
14. Tamboli V, Mishra GP, Mitra AK. Biodegradable polymers for ocular drug delivery. *Adv Ocul Drug Deliv*. 2012;2012:65–86.
15. Tamboli V, Mishra GP, Mitra AK. Polymeric vectors for ocular gene delivery. *Ther Deliv*. 2011;2(4):523–536.
16. Koo H, Moon H, Han H, et al. The movement of self-assembled amphiphilic polymeric nanoparticles in the vitreous and retina after intravitreal injection. *Biomaterials*. 2012;33(12):3485–3493.
17. Xu Q, Boylan NJ, Suk JS, et al. Nanoparticle diffusion in, and microrheology of, the bovine vitreous ex vivo. *J Control Release*. 2013; 167(1):76–84.
18. Shi S, Zhu X, Guo Q, et al. Self-assembled mPEG-PCL-g-PEI micelles for simultaneous codelivery of chemotherapeutic drugs and DNA: synthesis and characterization in vitro. *Int J Nanomedicine*. 2012;7: 1749–1759.
19. Shi S, Shi K, Tan L, et al. The use of cationic MPEG-PCL-g-PEI micelles for co-delivery of Msurvivin T34A gene and doxorubicin. *Biomaterials*. 2014;35(15):4536–4547.
20. Klimczak RR, Koerber JT, Dalkara D, Flannery JG, Schaffer DV. A novel adeno-associated viral variant for efficient and selective intravitreal transduction of rat Muller cells. *PLoS One*. 2009;4(10): e7467.

## International Journal of Nanomedicine

### Publish your work in this journal

The International Journal of Nanomedicine is an international, peer-reviewed journal focusing on the application of nanotechnology in diagnostics, therapeutics, and drug delivery systems throughout the biomedical field. This journal is indexed on PubMed Central, MedLine, CAS, SciSearch®, Current Contents®/Clinical Medicine,

Submit your manuscript here: <http://www.dovepress.com/international-journal-of-nanomedicine-journal>

Dovepress

Journal Citation Reports/Science Edition, EMBASE, Scopus and the Elsevier Bibliographic databases. The manuscript management system is completely online and includes a very quick and fair peer-review system, which is all easy to use. Visit <http://www.dovepress.com/testimonials.php> to read real quotes from published authors.